# A Fully-Decentralized Consensus-Based ADMM Approach for DC-OPF With Demand Response

Yamin Wang, *Student Member, IEEE*, Lei Wu, *Senior Member, IEEE*, and Shouxiang Wang, *Senior Member, IEEE*

***Abstract*—This paper discusses a consensus-based alternating direction method of multipliers (ADMMs) approach for solving the dynamic dc optimal power flow (DC-OPF) problem with demand response in a distributed manner. In smart grid, emerging techniques together with distributed nature of data and information, significantly increase the complexity of power systems operation and stimulate the needs for distributed optimization. In this paper, the distributed DC-OPF approach solves local OPF problems of individual subsystems in parallel, which are coordinated via global consensus variables (i.e., phase angles on boundary buses of adjacent subsystems). Three distributed DC-OPF algorithms are discussed with different convergence performance and/or communication requirement. All three distributed algorithms can effectively handle prevailing constraints for the transmission network, generating units, and demand response in individual subsystems, while the global convergence can be guaranteed. In particular, based on the traditional distributed ADMM approach, a fully decentralized algorithm without the central controller is proposed in Algorithm 2 with a new communication strategy, in which only limited information on boundary buses are exchanged among adjacent subsystems. In addition, the accelerated ADMM is discussed in Algorithm 3 for improving the convergence performance. In recognizing distributed OPF approaches in literature, one major research focus on this paper is to quantify the impact of key parameters and subsystem partitioning strategies on the convergence performance and the data traffic via numerical case studies. A general guidance for subsystem partitioning is proposed and verified via large-scale power systems.**

***Index Terms*—ADMM, demand response, distributed DC-OPF.**

## NOMENCLATURE

*Variables*

| | |
|---|---|
| $b, j, v$ | Indices of buses |
| $bj$ | Index of line from bus $b$ to bus $j$ |
| $d_{r,t}$ | Actual load level of demand $r$ in time period $t$ |
| $f_m(.)$ | Fuel cost of generator $m$ |
| $g(.)$ | Piecewise integral function of the price-demand curve |
| $i, t$ | Index of iterations/time periods |
| $m, r, n$ | Index of generation units/loads/subsystems |
| $P_{m,t}$ | Active power output of generator $m$ in time period $t$ |
| $\theta_{b,t}, \theta_{j,t}$ | Phase angles on bus $b$ and bus $j$ in time period $t$ |

*Constants*

| | |
|---|---|
| $d_{r,total}$ | Total load of demand $r$ in 24 hours |
| $d^0_{r,t}$ | Fixed load of demand $r$ in time period $t$ |
| $d^{\max}_{r,t}$ | Maximum value of demand $r$ in time period $t$ |
| $F^{\max}_{bj}$ | Maximum power flow limit on line $bj$ |
| $P^{\min}_m$,$P^{\max}_m$ | Minimum/maximum capacity of generator $m$ |
| $P^{up}_m$,$P^{down}_m$ | Ramp up/down rate limit of generator $m$ |
| $X_{bj}$ | Reactance of line $bj$ |
| $\theta_{ref,t}$ | Angle of the reference bus in time period $t$ |

*Vectors, Matrices, and Sets*

| | |
|---|---|
| $\boldsymbol{B}$ | Network admittance matrix |
| $\boldsymbol{D_t}$ | Vector of active power demands in time period $t$ |
| $\boldsymbol{L, M, T_r}$ | Set of load demands/ generating units/ lines |
| $\boldsymbol{N}$ | Set of subsystems |
| $\boldsymbol{P_t}$ | Vector of active power generations in time period $t$ |
| $\boldsymbol{T}$ | Set of time periods |
| $\boldsymbol{Z}$ | Set of global variables |
| $\boldsymbol{\theta}_t$ | Vector of bus angles in time period $t$ |

## I. INTRODUCTION

OPTIMAL power flow (OPF) determines the least-cost operation of power systems by dispatching generation resources to supply system loads, while satisfying prevailing system-level and unit constraints. DC-OPF is an approximation of AC-OPF for obtaining the optimal real power dispatch solution of the entire power system. This paper focuses on the dynamic DC-OPF problem with given unit commitment decisions, which is a widely used tool in day-ahead bulk power markets for determining the optimal scheduling of generating units and loads.

Emerging smart grid techniques are bringing new entities into power markets, including renewable generation owners as well as active customers equipped with self-owned generation resources and advanced metering infrastructures. These entities tend to autonomously maximize their own profits while they may not be willing to disclose actual financial information to system operators. Demand response (DR) is an important application in smart grid, which could enable

Manuscript received May 19, 2015; revised August 25, 2015 and December 15, 2015; accepted February 17, 2016. Date of publication March 8, 2016; date of current version October 19, 2017. This work was supported by the U.S. National Science Foundation under Grant ECCS-1254310. Paper no. TSG-00564-2015.

Y. Wang and L. Wu are with the Electrical and Computer Engineering Department, Clarkson University, Potsdam, NY 13699 USA (e-mail: yamwang@clarkson.edu; lwu@clarkson.edu).

S. Wang is with the Key Laboratory of Smart Grid of Ministry of Education, Tianjin University, Tianjin 300072, China.

Color versions of one or more of the figures in this paper are available online at http://ieeexplore.ieee.org.

Digital Object Identifier 10.1109/TSG.2016.2532467

the active interaction between end-users and the grid and reduce the needs for building new generation and transmission assets to supply peak demands [1]–[4]. However, DR is highly flexible and the central system operator may not respond quickly to the changes of DR. In view of these new features, a new research trend explores distributed optimization for various power systems applications, including distributed economic dispatch (ED) [5]–[8], distributed unit commitment [9], and distributed OPF [10], [11]. This paper focuses on the distributed optimization approach for the dynamic DC-OPF problem with DR. Comparing to the centralized OPF, the distributed OPF has following advantages:

1) The traditional centralized OPF requires high bandwidth communication infrastructures because all detailed information needs to be collected by the central controller. In comparison, in distributed OPF, smaller-scale local problems for individual subsystems are solved in a distributed manner and only limited information needs to be exchanged with adjacent subsystems and/or the central controller during the optimization procedure.

2) In the distributed OPF, individual subsystems do not need to disclose their confidential financial information to other subsystems and the central controller.

3) Distributed OPF is more scalable and flexible with respect to system changes than centralized operations, especially in view that topologies of electric power and communication infrastructures are more dynamic in smart grid.

4) Distributed OPF is more robust than centralized OPF. In the centralized optimization, the entire system could be disrupted when the central controller goes offline. On the other hand, distributed OPF can be solved asynchronously via individual local controllers [12]. That is, with the loss of certain local controllers, other local controllers can continue their normal functionalities. In addition, accurate result could be finally achieved once the lost local controllers come back online.

Over the past few years, various approaches have been explored for solving power system operation problems in a distributed fashion. One fundamental method is based on Lagrangian Relaxation (LR) [13]–[15]. In this method, coupling constraints among different subsystems are relaxed via Lagrangian multipliers and the derived problem becomes separable. A dynamic multiplier-based LR approach for solving ED in a fully decentralized manner was discussed in [16].

Many further established distributed optimization methods are based on LR. One popular approach is called auxiliary problem principle (APP) [17], which was applied to distributed OPF problems [18], [19]. APP can be interpreted as solving a sequence of auxiliary problems involving the augmented LR, for improving convergence performance of the standard LR. Recently, alternating direction method of multipliers (ADMM) has drawn more attentions, which is well suited for distributed convex optimization [20]–[24]. A compact formulation of ADMM was discussed in [23] for solving the AC-OPF problem. In [24], the OPF problem was formulated as a semi-definite programming problem and solved in a distributed fashion via ADMM.

Another important method applied to distributed optimization is the consensus algorithm. Distributed ED approach based on the incremental cost (IC) consensus was discussed in [5], [6], and [12]. However, only generator capacity limits are considered in [5] and [12]. Although transmission line losses are included in [6], other important factors such as transmission line capacity limits, generator ramp up/down limits, and DR may not be easily considered via this method. In [7], a fully decentralized ED approach with the flooding-based consensus algorithm was established. In the flooding consensus algorithm, data in one subsystem are sent to all other subsystems, which could exacerbate the communication bottleneck. A marginal equivalent based method was discussed in [8] for solving the linear dispatch problem, which requires significant information exchange including shift factors. In addition, consensus algorithm conjunct with ADMM was discussed in [26], and distributed consensus problem in the context of ADMM was established in [25].

This paper discusses a distributed DC-OPF approach by solving a global variable consensus problem via ADMM. As emphasized in [25], the application of ADMM is important and challenging. This paper introduces an effective way to properly match ADMM to the distributed DC-OPF problem. Different from the IC consensus based distributed algorithms in [5], [6], and [12], the proposed method can effectively handle prevailing constraints for the transmission network, individual generating units, and DR in individual subsystems. Different from ADMM based distributed algorithms in [22] and [24], the proposed method is a consensus like algorithm in conjunction with ADMM. In [22], data in one subsystem are sent to all other subsystems, while the proposed distributed DC-OPF approach only requires limited information exchange among adjacent subsystems, i.e., bus angle variables on boundary buses of adjacent subsystems. Furthermore, different from the Karush-Kuhn-Tucker optimality conditions decomposition based approach [27], [28], the proposed method based on ADMM can guarantee the global convergence. As stated in [28], although convergence properties seem to be satisfied in most practical cases, in certain cases the convergence criterion may not hold and modified decomposition method is required. On the other hand, as the DC-OPF model is a convex problem with linear constraints, the proposed approach can always guarantee the global convergence [25].

The major contributions of the paper are threefold.

1) Three distributed DC-OPF algorithms are discussed in this paper by leveraging the convergence performance as well as the information exchanged among subsystems and the central controller. In particular, a fully decentralized algorithm without the central controller is proposed in Algorithm 2 with a new communication strategy, in which only limited data on boundary buses are exchanged among adjacent subsystems. In addition, Algorithm 3 discusses an accelerated ADMM based distributed DC-OPF approach, at the cost of additional data exchange with the central controller. To the best knowledge of the authors, it is the first time that the accelerated ADMM is applied to the distributed optimization for power systems.

2) The proposed distributed algorithms can effectively handle a more realistic and complicated dynamic DC-OPF problem than those discussed in literature. That is, prevailing constraints for the transmission network, individual generating units, and DR in individual subsystems are considered, while the global convergence is guaranteed. In addition, the proposed distributed algorithms only require limited information exchange among adjacent subsystems, i.e., bus angle variables on boundary buses of adjacent subsystems. This feature helps reduce communication bottleneck and protect confidential financial information of individual subsystems.

3) One major research focus of this paper is to investigate how subsystem partitioning strategies and key parameters would impact the convergence performance of distributed optimization in power systems. When applying distributed optimization to large-scale power systems, an informative guidance on subsystem partition is very important for enhancing the computational performance. A useful indicator for the convergence performance of the proposed decentralized DC-OPF is the number of global variables. That is, fewer global variables usually mean less information exchange and a smaller number of iterations. Thus, a general guidance on subsystem partition is to involve fewer coupling nodes, which could reduce the number of global variables and enhance the convergence performance of the proposed decentralized DC-OPF approach. Case studies on large-scale power systems are presented to verify the proposed guidance on the subsystem partitioning.

The rest of this paper is organized as follows. Section II presents the formulation of the dynamic DC-OPF problem with DR. Section III discusses the proposed distributed DC-OPF approaches. Numerical case studies are presented in Section IV. Finally, Section V summarizes conclusions and plans for future research.

## II. Formulation of the Dynamic DC-OPF With DR

The dynamic DC-OPF problem is formulated as (1)-(13), which optimizes the day-ahead hourly schedule of generators and DR loads for maximizing the social welfare (1). (2) represents the nodal power balance restriction via the DC power flow calculation. (3) defines the reference bus. (4)-(5) are capacity limits of transmission lines and generators. (6)-(7) enforce ramp up/down limits of individual generators. (8) ensures lower and upper limits of each load demand, and (9) guarantees that the total energy requirement of each load is met after DR.

Quadratic function (10) is used to calculated the fuel cost of generators $f_m(P_{m,t})$, where $a_m^1$, $a_m^2$, and $a_m^3$ are constants for generator $m$. The piecewise price-demand curve function $g(d_{r,t})$ is used to represent the price elasticity of a DR load $r$ [29]. As shown in Fig. 1, each demand $r$ includes an inelastic load component $d_{r,t}^0$ that is insensitive to electricity prices, and an elastic load component that decreases with the price increase (i.e., segments from $d_{r,t}^0$ to $d_{r,t}^{\max}$). $g(d_{r,t})$ is calculated by (11)-(13), where $l_{r,t}^k$ is the $k$th step length of the step-wise function, $p_{r,t}^k$ is the price at step $k$, $h_{r,t}^k$ is the auxiliary variable of demand level at step $k$, and $\boldsymbol{K}$ is the set of steps.

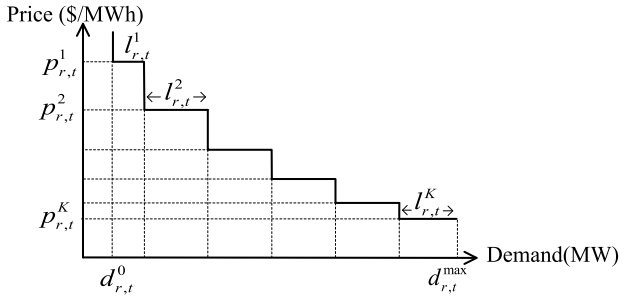


Fig. 1. The price-elastic demand curve.

The dynamic DC-OPF model (1)-(13), by co-optimizing the day-ahead hourly schedule of generators and DR loads for maximizing the social welfare, can effectively reflect the interaction between generators and DR loads. That is, the optimal schedule of DR loads depends on the operation cost of generators and vice versa. For instance, if the price of a DR load is higher than the marginal operation cost of a generator, dispatch of the generator will be increased for supplying the DR load and maximizing the social welfare. Otherwise, dispatch the generator will be decreased and DR load will not be supplied. Reference [29] used the similar DR formulation to investigate the impact of DR on power systems operation in day-ahead market.

$$\max\left(\sum_{t\in\boldsymbol{T}}\sum_{r\in\boldsymbol{L}} g\left(d_{r,t}\right) - \sum_{t\in\boldsymbol{T}}\sum_{m\in\boldsymbol{M}} f_m\left(P_{m,t}\right)\right) \tag{1}$$

$$\mathbf{B}\cdot\boldsymbol{\theta}_t = \mathbf{P}_t - \mathbf{D}_t \quad ,\forall t\in\boldsymbol{T} \tag{2}$$

$$\theta_{ref,t} = 0 \quad ,\forall t\in\boldsymbol{T} \tag{3}$$

$$\left|\left(\theta_{b,t}-\theta_{j,t}\right)/\mathrm{X}_{bj}\right| \le F_{bj,t}^{\max}, \quad \forall bj\in\boldsymbol{T}_r, \forall t\in\boldsymbol{T} \tag{4}$$

$$P_{m,t}^{\min} \le P_{m,t} \le P_{m,t}^{\max} \quad ,\forall m\in\boldsymbol{M}, \forall t\in\boldsymbol{T} \tag{5}$$

$$P_{m,t} - P_{m,(t-1)} \le P_m^{up}, \forall m\in\boldsymbol{M}, \forall t\in\boldsymbol{T} \tag{6}$$

$$P_{m,(t-1)} - P_{m,t} \le P_m^{down}, \forall m\in\boldsymbol{M}, \forall t\in\boldsymbol{T} \tag{7}$$

$$d_{r,t}^0 \le d_{r,t} \le d_{r,t}^{\max}, \forall r\in\boldsymbol{L}, \forall t\in\boldsymbol{T} \tag{8}$$

$$\sum_{t\in\boldsymbol{T}} d_{r,t} = d_{r,total}, \quad \forall r\in\boldsymbol{L} \tag{9}$$

$$f_m\left(P_{m,t}\right) = a_m^1\cdot\left(P_{m,t}\right)^2 + a_m^2\cdot P_{m,t} + a_m^3, \forall m\in\boldsymbol{M}, \forall t\in\boldsymbol{T} \tag{10}$$

$$g(d_{r,t}) = \sum_{k\in\boldsymbol{K}} p_{r,t}^k h_{r,t}^k, \forall r\in\boldsymbol{L}, \forall t\in\boldsymbol{T} \tag{11}$$

$$d_{r,t} = \sum_{k\in\boldsymbol{K}} h_{r,t}^k, \forall r\in\boldsymbol{L}, \forall t\in\boldsymbol{T} \tag{12}$$

$$0 \le h_{r,t}^k \le l_{r,t}^k, \forall k\in\boldsymbol{K}, \forall r\in\boldsymbol{L}, \forall t\in\boldsymbol{T}. \tag{13}$$

## III. Consensus-Based Distributed DC-OPF via ADMM

This section first introduces the standard ADMM algorithm, followed by the detailed discussion on reformulating the dynamic DC-OPF problem (1)-(13) into a suitable form that can apply ADMM for the distributed optimization. Three algorithms are presented and their communication strategies are discussed in details. Algorithm 1 is the ADMM based

distributed DC-OPF with the central controller. Algorithm 2 is a fully decentralized DC-OPF, in which local problems are solved in parallel and no central controller is required. Algorithm 3 presents an accelerated ADMM for improving the convergence performance. To facilitate the discussion, the algorithms are illustrated along with a small example.

### A. ADMM

ADMM [25] solves optimization problems in the form of (14)-(15), where $\boldsymbol{x} \in \mathbf{R}^{q_1}$, $\mathbf{z} \in \mathbf{R}^{q_2}$, $\mathrm{A}_1 \in \mathbf{R}^{q_3 \times q_1}$, $\mathrm{A}_2 \in \mathbf{R}^{q_3 \times q_2}$, and $\boldsymbol{c} \in \mathbf{R}^{q_3}$. $c_1(x)$ and $c_2(z)$ are convex functions of $\boldsymbol{x}$ and $\mathbf{z}$, respectively.

$$\min_{\boldsymbol{x},\boldsymbol{z}} \quad c_1(\boldsymbol{x}) + c_2(\mathbf{z}) \tag{14}$$

$$s.t. \quad \mathrm{A}_1 \cdot \boldsymbol{x} + \mathrm{A}_2 \cdot \boldsymbol{z} = \boldsymbol{c} \tag{15}$$

The augmented Lagrangian function of (14)-(15) is formed as (16), where $\lambda$ are Lagrangian multipliers of (15), $\rho > 0$ is a predefined parameter, and $\|.\|_2$ represents the $\ell_2$-norm of a vector. ADMM consists of the iterative procedure among (17)-(19), where $i$ is the index of ADMM iterations. Decision variables $\boldsymbol{x}$ and $\mathbf{z}$ are separately optimized in (17) and (18), which makes ADMM an efficient approach for distributed optimization.

$$\min_{\boldsymbol{x},\mathbf{z}} L_\rho(\boldsymbol{x}, \mathbf{z}, \boldsymbol{\lambda}) = c_1(\boldsymbol{x}) + c_2(\mathbf{z}) + \boldsymbol{\lambda}^T \cdot (\mathrm{A}_1 \cdot \boldsymbol{x} + \mathrm{A}_2 \cdot \mathbf{z} - \boldsymbol{c}) + (\rho/2) \cdot \|\mathrm{A}_1 \cdot \boldsymbol{x} + \mathrm{A}_2 \cdot \mathbf{z} - \boldsymbol{c}\|_2^2 \tag{16}$$

$$\boldsymbol{x}^{i+1} = \arg\min_{\boldsymbol{x}} L_\rho\left(\boldsymbol{x}, \mathbf{z}^i, \boldsymbol{\lambda}^i\right) \tag{17}$$

$$\mathbf{z}^{i+1} = \arg\min_{\mathbf{z}} L_\rho\left(\boldsymbol{x}^{i+1}, \mathbf{z}, \boldsymbol{\lambda}^i\right) \tag{18}$$

$$\boldsymbol{\lambda}^{i+1} = \boldsymbol{\lambda}^i + \rho \cdot \left(\mathrm{A}_1 \cdot \boldsymbol{x}^{i+1} + \mathrm{A}_2 \cdot \mathbf{z}^{i+1} - \boldsymbol{c}\right) \tag{19}$$

The convergence of ADMM is characterized in terms of the primal residual (20) and the dual residual (21), where $\varepsilon_1$ and $\varepsilon_2$ are predefined thresholds. The primal residual (20) is consistent with the definition of the primal residual in [25]. According to [25], the primal residual $r$ is calculated via primal variables $\boldsymbol{x}$ and $\mathbf{z}$ as shown in (22). The primal residual (20) is also based on primal variables $\boldsymbol{x}$ and $\mathbf{z}$, by recognizing that $\left(\boldsymbol{\lambda}^{i+1} - \boldsymbol{\lambda}^i\right)$ is a function of primal variables $\boldsymbol{x}$ and $\mathbf{z}$ according to (19). That is, substituting (19) into (20), the primal residual (20) can be equivalently transferred into a function of primal variables $\boldsymbol{x}$ and $\mathbf{z}$ as shown in (23). In comparison, (22) and (23) only differ by the predefined parameter $\rho$. In turn, the calculation of the primal residual (20) is mathematically consistent with the definition of $r$ in [25]. In addition, the expression (20) is concise and can keep consistent with the form of the dual residual (21).

$$\left\|\boldsymbol{r}^{i+1}\right\|_2^2 = \left\|\boldsymbol{\lambda}^{i+1} - \boldsymbol{\lambda}^i\right\|_2^2 \le \varepsilon_1 \tag{20}$$

$$\left\|\boldsymbol{s}^{i+1}\right\|_2^2 = \rho \cdot \left\|\mathbf{z}^{i+1} - \mathbf{z}^i\right\|_2^2 \le \varepsilon_2 \tag{21}$$

$$\boldsymbol{r}^{i+1} = A_1 \boldsymbol{x}^{i+1} + A_2 \mathbf{z}^{i+1} - \boldsymbol{c} \tag{22}$$

$$\left\|\boldsymbol{r}^{i+1}\right\|_2^2 = \left\|\boldsymbol{\lambda}^{i+1} - \boldsymbol{\lambda}^i\right\|_2^2 = \left\|\rho \cdot \left(\mathrm{A}_1 \cdot \boldsymbol{x}^{i+1} + \mathrm{A}_2 \cdot \mathbf{z}^{i+1} - \boldsymbol{c}\right)\right\|_2^2 \le \varepsilon_1 (20) \tag{23}$$

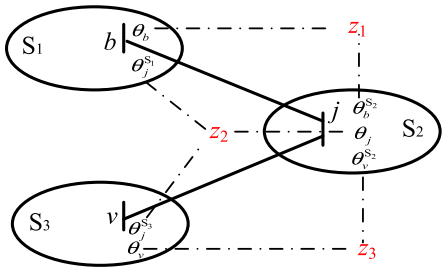


Fig. 2. A three-bus illustrative example.

### B. Reformulation of ADMM Based Distributed DC-OPF

The ADMM algorithm (14)-(15) includes two separable functions $c_1(\boldsymbol{x})$ and $c_2(\mathbf{z})$. However, most distributed optimization applications, such as the DC-OPF problem, may include multiple separable objective functions. ADMM based distributed optimization for solving multiple separable objective functions (24) is also analyzed in [25].

$$\min_{x,z} \sum_{n \in N} c_n(\boldsymbol{x}_n) + c_z(\mathbf{z})$$
$$s.t.\ \boldsymbol{x}_n - \mathbf{z} = 0, \quad \forall n \in N \tag{24}$$

A three-bus system shown in Fig. 2 is used as an example to illustrate the idea to transform the centralized DC-OPF problem into the form (24), so that ADMM can be applied to solve the DC-OPF problem in a distributed fashion. The system in Fig. 2 is decomposed into three subsystems $\mathrm{S}_1$, $\mathrm{S}_2$, and $\mathrm{S}_3$. Buses $b$, $j$, and $v$ are called boundary buses. Transmission line $bj$ connecting $\mathrm{S}_1$ and $\mathrm{S}_2$ and line $jv$ connecting $\mathrm{S}_2$ and $\mathrm{S}_3$ are called tie lines. Variables/constraints specified for each subsystem are called local variables/constraints of the subsystem.

The DC-OPF model established in Section II presents a peculiar structure with respect to local variables and local constraints. The objective function (1) for a subsystem is based on information of local generators and demands only. Constraints (5)-(9) are also based on local variables. On the other hand, subsystems are coupled with each other via power flows on tie lines. Thus, constraints (2) and (4) containing power flows of tie lines are not naturally separable. For instance, in $\mathrm{S}_2$, local power balance equation on the boundary bus $j$ includes power flows of tie lines $bj$ and $vj$ written as $F_{bj}$ and $F_{vj}$. $F_{bj}$ is calculated by $\left(\theta_b - \theta_j\right)/x_{bj}$, which includes variable $\theta_b$ belonging to subsystem $\mathrm{S}_1$. Similarly, $F_{vj}$ needs $\theta_v$ that belongs to $\mathrm{S}_3$.

To bring (2) and (4) into a suitable form for the ADMM based distributed optimization, in the proposed algorithm, phase angles of boundary buses in one subsystem are duplicated in its adjacent subsystems. For instance, in Fig. 2, $\theta_j$ in subsystem $\mathrm{S}_2$ is duplicated in adjacent subsystems $\mathrm{S}_1$ and $\mathrm{S}_3$ as $\theta_j^{S_1}$ and $\theta_j^{S_3}$, respectively. Similarly, $\theta_b$ in $\mathrm{S}_1$ is duplicated in $\mathrm{S}_2$ as $\theta_b^{S_2}$, and $\theta_v$ in $\mathrm{S}_3$ is duplicated in $\mathrm{S}_2$ as $\theta_v^{S_2}$. For each subsystem, phase angle variables of boundary buses and variables duplicated from other subsystems are called coupling variables. Thus, by duplicating boundary bus angle variables, (2) and (4) can be transformed into functions of local variables and coupling variables.

In the proposed distributed algorithm, global variables $\mathbf{z}$ link the same variables duplicated in different subsystems. For instance, in Fig. 2, $z_1$ bundles $\theta_b$ and $\theta_b^{S_2}$, Similarly, $\theta_j^{S_1}$, $\theta_j$, and $\theta_j^{S_3}$ correspond to $z_2$, while $\theta_v$ and $\theta_v^{S_2}$ correspond to $z_3$. (25)-(27) are included in subsystems $S_1$, $S_2$, and $S_3$ respectively, which guarantee that the same variables duplicated in different subsystems are equal to each other.

$$\theta_b - z_1 = 0, \quad \theta_j^{S_1} - z_2 = 0 \tag{25}$$

$$\theta_b^{S_2} - z_1 = 0, \ \theta_j - z_2 = 0, \ \theta_v^{S_2} - z_3 = 0 \tag{26}$$

$$\theta_j^{S_3} - z_2 = 0, \ \theta_v - z_3 = 0 \tag{27}$$

With the above illustration, the dynamic DC-OPF model (1)-(13) can be reformulated in a separable form that is suitable for the distributed optimization. For the sake of discussion, variables of subsystem $n$ are expressed as $\boldsymbol{x}_n$, which include local variables $\bar{\boldsymbol{x}}_n$ and coupling variables $\tilde{\boldsymbol{x}}_n$. Local variables $\bar{\boldsymbol{x}}_n$ include generation dispatches, demand levels of DR loads, and bus angles in subsystem $n$ except boundary buses. Coupling variables $\tilde{\boldsymbol{x}}_n$ include phase angle variables of boundary buses in subsystem $n$ and duplicated phase angle variables of boundary buses in adjacent subsystems. For instance, in Fig. 2, $\tilde{\boldsymbol{x}}_{S_1}$ for subsystem $S_1$ include $\theta_b$ and $\theta_j^{S_1}$.

For the distributed DC-OPF problem, the objective of the entire system (1) can be represented as the summation of objectives for individual subsystems (28), where $C_n(\boldsymbol{x}_n)$ represents the objective function of subsystem $n$. $\boldsymbol{x}_n$ satisfying (2)-(13) in subsystem $n$ is represented as $\boldsymbol{x}_n \in \chi_n$ in (29). Constraint (30) guarantees that the same variables expressed in different subsystems are equal to each other, where $\mathbf{z}_n$ represent global variables corresponding to subsystem $n$. For instance, for subsystem $S_1$ in Fig. 2, $\mathbf{z}_{S_1}$ include $z_1$ and $z_2$, and (30) for $S_1$ represents the two constraints in (25). (28)-(30) present a separable DC-OPF formulation with the similar form as (24), which is suitable for the distributed optimization via ADMM.

$$\min \quad \sum_{n \in N} C_n(\boldsymbol{x}_n) \tag{28}$$

$$s.t. \quad \boldsymbol{x}_n \in \boldsymbol{\chi}_n, \qquad \forall n \in \boldsymbol{N} \tag{29}$$

$$\tilde{\boldsymbol{x}}_n - \mathbf{z}_n = 0, \qquad \forall n \in \boldsymbol{N} \tag{30}$$

(31) is the augmented Lagrangian function of (28), where $\lambda_n$ are Lagrangian multipliers corresponding to (30) and $\rho$ is a predefined positive parameter. The $i^{th}$ iteration of the distributed DC-OPF process includes three steps of (32)-(34). (32) for individual subsystems can be solved in parallel. (33) means that the global variable $z_g$ equals to the average of all $(\tilde{\boldsymbol{x}}_n)_w$ that correspond to $z_g$. $(\tilde{\boldsymbol{x}}_n)_w$ represents the $w^{\text{th}}$ variable of $\tilde{\boldsymbol{x}}_n$. The mapping from duplicated coupling variables $\tilde{\boldsymbol{x}}_n$ onto the global variable $\mathbf{z}_n$ is written as $g{=}G(n,w)$. That is, $(\tilde{\boldsymbol{x}}_n)_w$ corresponds to the global variable $z_g$. For instance, in Fig 2, the global variable $z_2$ can be updated via (35). The algorithm stops when primal and dual residuals (36) in each subsystem $n$ are sufficiently small.

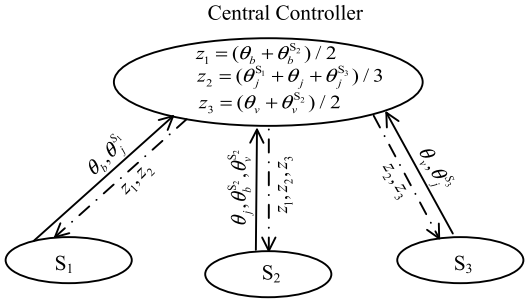


Fig. 3. Illustration of Algorithm 1 applied on the example.

$$\min_{\boldsymbol{x},\mathbf{z}} L_\rho(\boldsymbol{x}, \mathbf{z}, \lambda) = \sum_{n=1}^{N} \Big[ C_n(\boldsymbol{x}_n) + \boldsymbol{\lambda}_n^T \cdot (\tilde{\boldsymbol{x}}_n - \mathbf{z}_n) + (\rho/2) \cdot \|\tilde{\boldsymbol{x}}_n - \mathbf{z}_n\|_2^2 \Big] \tag{31}$$

$$\boldsymbol{x}_n^{i+1} = \arg\min_{\boldsymbol{x}_n \in \chi_n} \Big( C_n(\boldsymbol{x}_n) + \boldsymbol{\lambda}_n^{iT} \cdot \boldsymbol{x}_n + (\rho/2) \cdot \big\|\tilde{\boldsymbol{x}}_n - \mathbf{z}_n^i\big\|_2^2 \Big), \forall n \in \boldsymbol{N} \tag{32}$$

$$\mathbf{z}_g^{i+1} = \frac{\sum_{G(n,w)=g} \big(\tilde{x}_n^{i+1}\big)_w}{\sum_{G(n,w)=g} 1}, \forall g \in \boldsymbol{Z} \tag{33}$$

$$\boldsymbol{\lambda}_n^{i+1} = \boldsymbol{\lambda}_n^i + \rho \cdot \Big( \tilde{\boldsymbol{x}}_n^{i+1} - \mathbf{z}_n^{i+1} \Big), \forall n \in \boldsymbol{N} \tag{34}$$

$$z_2 = \Big( \theta_j^{S_1} + \theta_j + \theta_j^{S_3} \Big)/3 \tag{35}$$

$$\Big\| \boldsymbol{r}_n^{i+1} \Big\|_2^2 = \Big\| \boldsymbol{\lambda}^{i+1} - \boldsymbol{\lambda}^i \Big\|_2^2 \le \varepsilon_1, \ \Big\| \boldsymbol{s}_n^{i+1} \Big\|_2^2 = \rho \cdot \Big\| \mathbf{z}_n^{i+1} - \mathbf{z}_n^i \Big\|_2^2 \le \varepsilon_2 \tag{36}$$

An efficient communication strategy is needed for the iterative procedure (32)-(34). The data exchange strategy and the detailed procedure are discussed in the next section.

### C. Procedure of the ADMM Based Distributed DC-OPF

*1) Distributed DC-OPF With the Central Controller:* The conventional communication strategy of distributed ADMM is based on the central controller. In this method, coupling variables of individual subsystems are sent to the central controller. The central controller calculates the global variable $z_g$ via (33), and sends updated $\mathbf{z}_n$ back to each subsystem $n$. After receiving $\mathbf{z}_n$, local operator in each subsystem $n$ calculates $\lambda_n$ via (34). The communication strategy for the example in Fig. 2 is illustrated in Fig. 3. Detailed procedure of ADMM based distributed DC-OPF with the central controller is described in Algorithm 1.

*2) ADMM Based Fully Decentralized DC-OPF Algorithm:* A new communication strategy is proposed to obtain a fully decentralized DC-OPF approach. The original phase angle variables (not the duplicated ones) corresponding to $z_g$ are called the leading variables, and the subsystem where the leading variables are located at is called the leading subsystem. For instance, in the example in Fig. 2, leading variables corresponding to $z_1$, $z_2$, and $z_3$ are $\theta_b$, $\theta_j$, and $\theta_v$, respectively,

**Algorithm 1** ADMM Based Distributed DC-OPF With the Central Controller

1. Initialize $\boldsymbol{\lambda}_n$ and $\mathbf{z}_n$ for each $n \in \boldsymbol{N}$.
2. Each subsystem $n \in \boldsymbol{N}$ solves the local DC-OPF problem (32).
3. Each subsystem $n \in \boldsymbol{N}$ sends $\tilde{\boldsymbol{x}}_n$ to the central controller.
4. The central controller updates $z_g$ via (33) for each $g \in \boldsymbol{Z}$.
5. The central controller sends $\mathbf{z}_n$ to each subsystem $n \in \boldsymbol{N}$.
6. If stopping criteria (36) are satisfied in all subsystems, the algorithm stops. Otherwise, each subsystem $n \in \boldsymbol{N}$ solves (34) locally for updating $\boldsymbol{\lambda}_n$ and goes to Step 2.

**Algorithm 2** ADMM Based Fully Decentralized DC-OPF

1. Initialize $\boldsymbol{\lambda}_n$ and $\mathbf{z}_n$ for each $n \in \boldsymbol{N}$.
2. Each subsystem $n \in \boldsymbol{N}$ solves the local DC-OPF problem (32).
3. Duplicated variables corresponding to $z_g$ are sent to the leading subsystem of $z_g$.
4. Leading subsystem of $z_g$ receives duplicated variables corresponding to $z_g$, and updates $z_g$ via (33).
5. Leading subsystem sends updated $z_g$ to corresponding adjacent subsystems.
6. If stopping criteria (36) are satisfied in all subsystems, the algorithm stops. Otherwise, each subsystem $n \in \boldsymbol{N}$ solves (34) locally for updating $\boldsymbol{\lambda}_n$ and goes to Step 2.

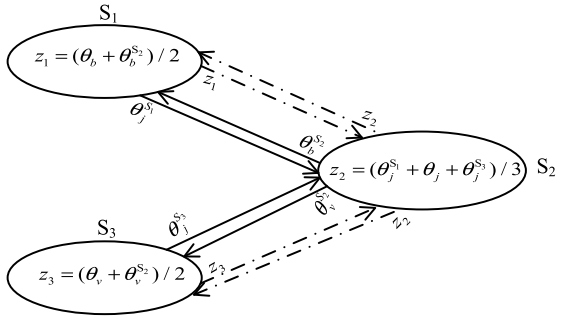


Fig. 4. Illustration of Algorithm 2 applied on the example.

and leading subsystem are $S_1$, $S_2$, and $S_3$, respectively. In the proposed data exchange strategy, values of duplicated variables corresponding to $z_g$ are sent to the leading subsystem of $z_g$.The local operator of the leading subsystem calculates the global variable $z_g$ via (33), and sends updated $z_g$ back to corresponding subsystems. The communication procedure of the example is illustrated in Fig. 4. Fig. 4 shows that the data exchange requirement of Algorithm 2 is much smaller than that of Algorithm 1, which could significantly reduce the communication bottleneck. Detailed procedure of the fully decentralized DC-OPF is described in Algorithm 2.

### *D. Distributed DC-OPF Based on Accelerated ADMM*

Accelerated ADMM is proposed in [30] recently. It is based on the work of Nesterov [31], which presents a general algorithm for accelerating gradient decent algorithms when solving convex optimization problems. In accelerated ADMM, extra steps (37)-(39) are added for updating $\mathbf{z}_g^{i+1}$ in (33) and

**Algorithm 3** Accelerated ADMM for Distributed DC-OPF

1. Initialize $\boldsymbol{\lambda}_n$ and $\mathbf{z}_n$ for each subsystem $n \in \boldsymbol{N}$.
2. Each subsystem $n \in \boldsymbol{N}$ solves the local ED problem (32).
3. Duplicated variables corresponding to $z_g$ are sent to the leading subsystem of $z_g$.
4. Leading subsystem of $z_g$ receives duplicated variables and updates $z_g$ via (33).
5. Leading subsystem sends updated $z_g$ to corresponding adjacent subsystems.
6. If stop criteria (36) are satisfied in all subsystems, algorithm stops. Otherwise,
   - 6.1. Each subsystem $n \in \boldsymbol{N}$ solves (34) locally.
   - 6.2. Each subsystem $n \in \boldsymbol{N}$ sends $\boldsymbol{r}_n$ and $\boldsymbol{s}_n$ to the central coordinator, and $\alpha$ is calculated via (39) by the central coordinator.
   - 6.3. The central coordinator broadcasts $\alpha$ to all subsystems.
   - 6.4. Subsystem $n$ receives $\alpha$, and updates $\mathbf{z}_n$ and $\boldsymbol{\lambda}_n$ by (37)-(38).
   - 6.5. Go to Step 2.

$\lambda_n^{i+1}$ in (34). Parameter $\alpha^i$ in (37)-(38) is defined in (39), where $\beta^1$=1 and $\beta^i = [1 + \sqrt{1 + 4(\beta^{i-1})^2}]/2$ for $i > 1$. Note that $\boldsymbol{r}$ and $\boldsymbol{s}$ in (39) are summations of primal and dual residuals for all subsystems. Thus, a central coordinator is needed in Algorithm 3 for calculating $\alpha^i$. The procedure of the accelerated ADMM- based distributed DC-OPF is concluded in Algorithm 3.

$$\hat{\mathbf{z}}_g^{i+1} = \alpha^i \cdot \mathbf{z}_g^{i+1} + \left(1 - \alpha^i\right) \cdot \mathbf{z}_g^i \tag{37}$$

$$\hat{\boldsymbol{\lambda}}_n^{i+1} = \alpha^i \cdot \boldsymbol{\lambda}_n^{i+1} + \left(1 - \alpha^i\right) \cdot \boldsymbol{\lambda}_n^i \tag{38}$$

$$\alpha^i = \begin{cases} 1 + \dfrac{\beta^i - 1}{\beta^{i+1}} & if \dfrac{\max\left(\left\|\boldsymbol{r}^i\right\|_2, \left\|\boldsymbol{s}^i\right\|_2\right)}{\max\left(\left\|\boldsymbol{r}^{i-1}\right\|_2, \left\|\boldsymbol{s}^{i-1}\right\|_2\right)} < 1 \\ 1 & otherwise \end{cases} \tag{39}$$

## IV. Numerical Case Studies

The proposed distributed DC-OPF algorithms are tested on a 6-bus system, the IEEE 118-bus system, and two 944-bus systems. The 6-bus system is used to quantify the impacts of parameter $\rho$ and the number of global variables on the convergence performance and the solution accuracy of the distributed DC-OPF algorithms. The IEEE 118-bus system case study focuses on the impact of the number of subsystems on convergence performance and communication efficiency of the three algorithms. To further verify the subsystem partitioning guidance obtained in the IEEE 118-bus system on larger systems, two 944-bus systems are tested via Algorithm 2. All proposed algorithms are implemented in MATLAB. Centralized DC-OPF problem and (32) for each subsystem $n$ are solved by CPLEX. Note that the only difference between Algorithms 1 and 2 is the communication strategy, and Algorithm 3 accelerates the convergence performance of ADMM at the cost of extra communication requirements. That is, final optimal solutions of the three algorithms would be the same. Thus, the solutions from

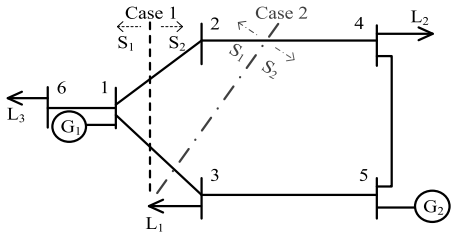


Fig. 5. 6-bus system.

TABLE I
GENERATOR INFORMATION

| Unit | $P^{\min}$ (MW) | $P^{\max}$ (MW) | $a^1$ ($/MW$^2$ h) | $a^2$ ($/MW h) | $a^3$ ($/h) |
|---|---|---|---|---|---|
| $G_1$ | 20 | 200 | 0.67 | 26.24 | 31.67 |
| $G_2$ | 50 | 200 | 0.11 | 12.89 | 6.78 |

TABLE II
BRANCH INFORMATION

| Branch | From | To | X (p.u.) | $F^{\max}$ (MW) |
|---|---|---|---|---|
| 1 | 1 | 2 | 0.6 | 150 |
| 2 | 1 | 3 | 0.6 | 150 |
| 3 | 2 | 4 | 0.1 | 150 |
| 4 | 3 | 5 | 0.1 | 150 |
| 5 | 4 | 5 | 0.1 | 150 |
| 6 | 1 | 6 | 0.1 | 150 |

TABLE III
TWO CASES FOR THE 6-BUS SYSTEM

| Case | Subsystems $S_n$ | Tie lines | # of global variables |
|---|---|---|---|
| 1 | $S_1$={1,6}<br>$S_2$={2,3,4,5} | Branches 1 and 2 | 3 |
| 2 | $S_1$={1,2,6}<br>$S_2$={3,4,5} | Branches 2 and 3 | 4 |

Algorithm 2 are used to evaluate the solution accuracy of the distributed DC-OPF, and convergence performance and communication efficiency of all three algorithms are evaluated.

### A. 6-Bus System

The 6-bus system includes 2 generators and 3 loads as shown in Fig. 5. Data for generators and transmission lines are given in Tables I-II, respectively. For the sake of discussion, in this case study, the system is studied for one hour and only inelastic demands are considered. $L_1$ on bus 3 and $L_2$ on bus 4 are both 150 MW, and $L_3$ on bus 6 is 10MW.

Two cases in Table III are studied. In Case 1, the system is partitioned into two subsystems via tie lines 1 and 2. In Case 2, the system is partitioned by tie lines 2 and 3. Algorithm 2 is applied on the 6-bus system, for investigating the impact of parameter $\rho$ on the convergence performance.

Convergence rates of the two cases with different values of $\rho$ are shown in Table IV, with $\varepsilon_1$ and $\varepsilon_2$ of $10^{-4}$. Results in Table IV show that improper $\rho$ could lead to a slow convergence. In addition, with the same $\rho$ the convergence performance of the two cases could be different. Thus, it may be impossible to define a unique value of $\rho$ that would be suitable for all practical problems [32]. Our experience shows

TABLE IV
IMPACT OF $\rho$ ON THE CONVERGENCE RATE

| $\rho$ | 2 | 4 | 8 | 10 | 20 | 50 | 100 |
|---|---|---|---|---|---|---|---|
| # of iterations in Case 1 | 285 | 139 | **49** | 59 | 103 | 160 | 209 |
| # of iterations in Case 2 | 3096 | 1536 | 740 | 597 | **278** | 566 | 963 |

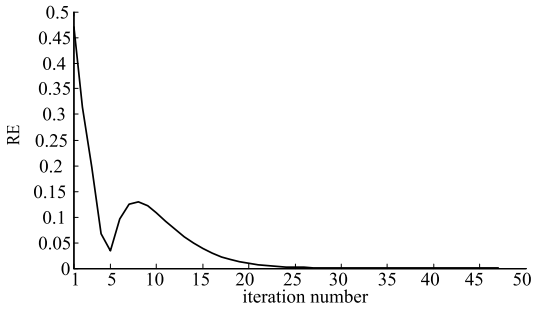


Fig. 6. Iterative values of RE in Case 1 with $\rho$ of 8 and $\varepsilon_1/\varepsilon_2$ of $10^{-4}$.

that $\rho$ in the range of 8-20 is usually proper for the distributed DC-OPF problem.

Results in Table IV also show that the number of global variables would impact the convergence performance. As shown in Fig. 5, the only difference between the two cases is that bus 2 belongs to subsystem 2 in Case 1, while it is contained in subsystem 1 in Case 2. In turn, Case 1 includes three global variables corresponding to phase angles of the three boundary buses 1-3, while Case 2 includes four global variables corresponding to phase angles of the four boundary buses 1-4. Results in Table IV show that for each $\rho$, the number of iterations in Case 1 is smaller than that in Case 2. In addition, the best performance in Case 1 is 49 iterations with $\rho$ of 8, which is significantly smaller than the best performance of 278 iterations with $\rho$=20 in Case 2. The major driven of the different performance is the essence of (33) for accomplishing the global variable consensus. Thus, a smaller number of global variables usually means less information exchange and less iteration. Thus, a useful guidance for partitioning the entire system into subsystems is the number of global variables. To achieve fewer global variables, the subsystem partition should involve fewer coupling buses. For instance, in this 6-bus case study, it is better to put bus 2 in subsystem 2.

The final optimal solution of the centralized DC-OPF method (1)-(13) is $P_{G1}$=110MW and $P_{G2}$=200MW. Relative error (RE) of generation dispatches (40) is used to evaluate the quality of distributed DC-OPF solutions, where $P_m^*$ and $P_m$ are dispatch results of generator $m$ from the centralized DC-OPF method and Algorithm 2, respectively. Table V shows the relationship between convergence thresholds and RE in Case 1 with $\rho$ of 8. RE in each iteration of Case 1 with $\varepsilon_1$ and $\varepsilon_2$ of $10^{-4}$ and $\rho$ of 8 is plotted in Fig. 6, which shows the iterative convergence performance of Algorithm 2. Table V indicates that higher solution accuracy requires a larger number of iterations. In addition, the proposed distributed DC-OPF algorithms can achieve good enough solution accuracy within a few tens of iterations. For instance, RE in Fig. 6 is reduced to $10^{-3}$ in 27 iterations. Thus, the proposed distributed algorithms are practically efficient when good enough accuracy is sufficient

TABLE V
RELATIONSHIP BETWEEN $\varepsilon$ AND RE IN CASE 1

| $\varepsilon_1/\varepsilon_2$ | $10^{-2}$ | $10^{-3}$ | $10^{-4}$ | $10^{-5}$ |
|---|---|---|---|---|
| RE | $7.84\times10^{-5}$ | $5.14\times10^{-6}$ | $5.22\times10^{-7}$ | $4.57\times10^{-9}$ |
| # of iterations | 37 | 44 | 49 | 54 |

TABLE VI
THREE CASES FOR THE IEEE 118-BUS SYSTEM

| Case | Subsystems $S_n$ | # of global variables |
|---|---|---|
| 1 | $S_1$={1-32,113-115,117}<br>$S_2$={33-73,116}<br>$S_3$={74-112,118} | 15×24(h)=360 |
| 2 | $S_1$={1-7,11-15,33-37,39-64,117}<br>$S_2$={8-10,16-32,38,65-82,96-99, 113-116,118}<br>$S_3$={83-95,100-112} | 26×24(h)=624 |
| 3 | $S_1$={1-32,113-115,117}<br>$S_2$={33-67}<br>$S_3$={68-81,116,118}<br>$S_4$={82-112} | 21×24(h)=504 |

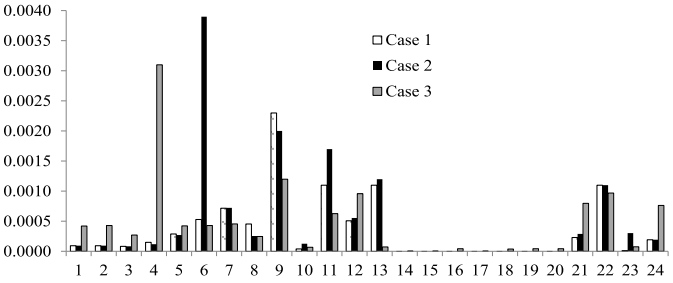


Fig. 7. Solution Accuracy Analysis of Algorithm 2.

from engineer point of view.

$$\mathrm{RE} = \sqrt{\sum_{m\in M}\left[\left(P_m^* - P_m\right)/P_m^*\right]^2} \tag{40}$$

### B. The IEEE 118-Bus System

The IEEE 118-bus system is tested for a 24-hour period via three cases as shown in Table VI. In Cases 1 and 2, the original 118-bus system is partitioned into 3 subsystems with 360 and 624 global variables, respectively, and is partitioned into 4 subsystems with 504 global variables in Case 3. Price-demand curves with eight piece-wise segments are considered for individual DR loads. The detailed data for the IEEE 118-bus system can be found in [33]. For all case studies, $\rho$ is set as 12, and $\varepsilon_1$ and $\varepsilon_2$ are 0.01.

Fig. 7 shows 24-hour REs of Algorithm 2 for illustrating its solution accuracy. Note that the final optimal solutions from the three algorithms are the same, so only results from Algorithm 2 are reported in Fig. 7. Fig. 7 shows that high accuracy can be achieved in all three cases.

To compare the convergence performance of Algorithms 2 and 3, iterative logarithmic values of RE at hour 1 in Case 1 are shown in Fig. 8. It indicates that the convergence rate of Algorithm 3 is accelerated as compared to Algorithm 2.

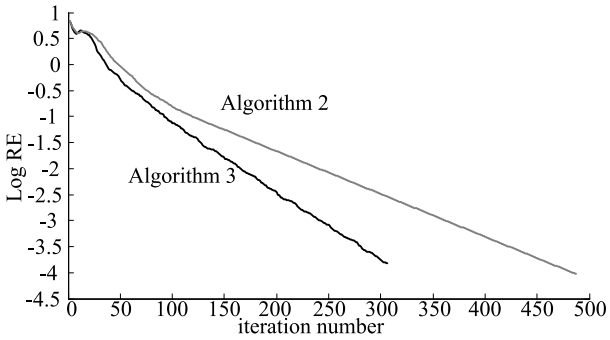


Fig. 8. Iterative logarithmic values of RE in Case 1.

TABLE VII
COMPARISON OF THE THREE PROPOSED DISTRIBUTED ALGORITHMS

| Case | 1 | | | 2 | | | 3 | | |
|---|---|---|---|---|---|---|---|---|---|
| Algorithm | 1 | 2 | 3 | 1 | 2 | 3 | 1 | 2 | 3 |
| # of iteration | 488 | 488 | 307 | 2126 | 2126 | 1957 | 792 | 792 | 621 |
| # of exchanged information unit per iteration | 70 | 40 | 102 | 116 | 64 | 142 | 94 | 56 | 134 |

To compare communication efficiency of the three proposed distributed algorithms, numbers of information units exchanged in the distributed optimization procedure are compared. One information unit is defined as transforming 24 values of one variable for the 24 hours (i.e., the phase angle of a boundary bus) from one subsystem to another. Note that information units exchanged in Algorithm 3 also include $\boldsymbol{r}_n$ and $\boldsymbol{s}_n$ that are sent from subsystems to the central controller. Table VII reports the number of iterations and the communication requirement of the three algorithms. It shows that numbers of information units exchanged per iteration in Algorithm 2 are smaller than those of Algorithms 1 and 3, which indicates that Algorithm 2 is a more communicational efficient method. When the problem scale is large, the computation time in each iteration could be more significant than the communication time. Thus, although the number of information units exchanged in Algorithm 3 is larger than that of Algorithm 2, the smaller total number of iterations in Algorithm 3 would reduce the total computational time of the distributed DC-OPF for large-scale power systems. Results of the three cases also show that the convergence performance largely depends on the way the system is partitioned. Specifically, it depends more on the number of global variables rather than the number of subsystems. Numbers of subsystems in Cases 1 and 2 are the same but they partition the system differently with different numbers of global variables. Results show that the convergence performance in Case 1 is much better than Case 2 because of the smaller number of global variables. In addition, although the number of subsystems in Case 3 is larger than that of Case 2, the number of global variables in Case 3 is smaller than that of Case 2. Thus, results indicate that Case 3 converges faster than Case 2.

The number of iterations and the computational time of individual subsystems are the two major factors that would impact the computational performance of the proposed distributed algorithms. In terms of the computational time of individual

subsystems, the best situation would be that all subsystems could finish their local computations simultaneously. That is, faster subsystem does not need to wait for slower ones. However, practical case studies show that for the DC-OPF problem, the difference in the computational time of individual subsystems is not significant in a single iteration, and the number of iterations is the major driven that impacts the total computational time. The reason is that the DC-OPF problem is a convex linear programming (LP) problem, and the-state-of-the-art LP solvers could solve subproblems of individual subsystems very fast. For instance, in a single iteration of the 6-bus case study, computational times of (32) for individual subsystems in both cases are all around 0.003s. That is, the difference in the computational time of individual subsystems is insignificant for a single iteration. As shown in Table IV, the total iterations of Cases 1 and 2 are 49 and 278, and the total computational times are 0.162s and 0.935s, which indicate that Case 1 is more computationally efficient than Case 2. As for the IEEE 118-bus system, total computational times of Cases 1-3 are 78.08s, 347.73s, and 92.87s, respectively, which also indicate that the number of iterations is the major factor that impacts the computational performance of the proposed distributed algorithms. Thus, a general guidance for subsystem partitioning is to involve fewer coupling nodes, which could reduce the number of global variables and enhance the convergence performance of the proposed distributed DC-OPF approaches.

From the above case studies, some features of Algorithm 2 over Algorithms 1 and 3 can be concluded.

1) Algorithm 2 is a fully decentralized algorithm without the central controller, as compared to Algorithms 1 and 3. The fully decentralized algorithm is more flexible and robust in response to system changes, since no detailed data need to be collected at the central controller.

2) Only limited data on boundary buses are exchanged among adjacent subsystems. The volume of data exchanged in Algorithm 2 is much smaller than those of Algorithms 1 and 3, which can help reduce the communication bottleneck.

### C. Large-Scale System Evaluation

As observed in Section IV-B, a general guidance for subsystem partitioning is to involve fewer coupling nodes, which would reduce the number of global variables and accelerate the convergence performance. To further verify this subsystem partitioning guidance, two 944-bus systems are tested via Algorithm 2 as shown in Fig. 9. Both systems include 8 subsystems and each subsystem is identical to the IEEE 118-bus system used in Section IV-B. In Case 1 the subsystems are connected by 7 tie lines while Case 2 includes 11 tie lines. In both cases, $\rho$ is set as 2, and $\varepsilon_1$ and $\varepsilon_2$ are 0.01.

The number of iterations and the total computational time are summarized in Table VIII. Results in Table VIII indicate that the number of iterations in Case 1 is much smaller than that of Case 2. This again verifies that fewer coupling nodes and in turn a smaller number of global variables would reduce the number of iterations. Furthermore, the number of iterations in Case 1 of Table VIII is even smaller than that of Case 1 in Table VI for the 118-bus system. It indicates that the convergence performance in terms of the number of iterations does not necessarily depend on the number of subsystems or the scale of power systems. On the other hand, the computational time of individual subsystems in a large-scale system is much longer than that of a small-scale system. In Cases 1-2, the computational time of individual subsystems (i.e., each subsystem is equivalent to the IEEE 118-bus system) is around 1.7s. Since the total computational time depends on the computational time of individual subsystems as well as the number of iterations, the proposed subsystem partition strategy would be important for reducing the number of iterations and enhancing the convergence performance of distributed DC-OPF approaches, especially when applied to large-scale power systems.

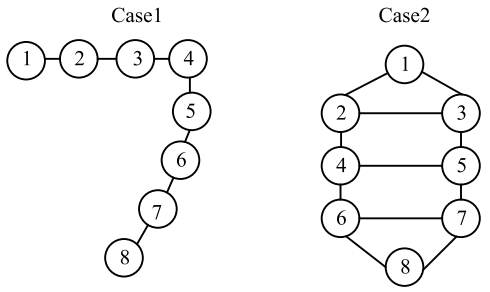


Fig. 9. Two 944-bus systems with 8 subsystems.

TABLE VIII
RESULTS OF TWO 944-BUS SYSTEMS

| Case | # of global variables | # of iterations | Computational time (s) |
|---|---|---|---|
| 1 | 14×24(h)=336 | 436 | 836 |
| 2 | 22×24(h)=528 | 1524 | 2704 |

## V. CONCLUSION

This paper discusses three ADMM-based distributed optimization algorithms for solving the dynamic DC-OPF problem with DR. The dynamic DC-OPF with DR is formulated as a convex problem with linear constraints. Solution accuracy, convergence performance, and communication requirement of the three proposed distributed algorithms are studied in numerical case studies. Algorithm 2 is a fully decentralized method without the central controller, which requires less data exchange among subsystems as compared to Algorithms 1 and 3. Accelerated ADMM applied in Algorithm 3 shows that the convergence performance can be enhanced at the cost of additional data exchanged with the central controller. As compared to distributed OPF approaches in literature, one major research focus on this paper is to quantify the impact of key parameters and subsystem partition strategies on the convergence performance and the data traffic. Results show that the convergence performance largely depends on the number of global variables rather than the number of subsystems or the scale of power systems. Thus, an effective subsystem partition strategy would be important for enhancing the convergence performance of distributed DC-OPF approaches, especially when applied to large-scale power systems.

This paper mainly focuses on decentralized algorithms for the deterministic DC-OPF problem with DR. The proposed distributed algorithms may be extended for solving DC-OPF problems with uncertainty, depending on the optimization approach being adopted, since ADMM can only guarantee the global convergence for convex problems [25]. Stochastic optimization and robust optimization are two widely used methods for handling optimization problems of power systems with uncertainties. Since scenario based stochastic DC-OPF model is still convex [34], the proposed decentralized algorithms may be directly used and the global convergence can be guaranteed. On the other hand, the proposed decentralized algorithms may not guarantee the global optimality when it is directly applied to the robust optimization based DC-OPF model, as robust optimization based models usually involve a second-stage maximin problem which makes the entire problem non-convex [35]. Furthermore, considering correlations of uncertainty factors across multiple subsystems will introduce additional coupling constraints among subsystems and may complicate decentralized algorithms. The application of the proposed decentralized algorithms for solving DC-OPF problems with uncertainty will be investigated in authors' future work.

Since DC-OPF is a convex problem with linear constraints, the proposed consensus-based ADMM algorithms can guarantee the global convergence. The application of the proposed distributed consensus-based ADMM algorithms to non-convex power systems problems, such as AC-OPF and unit commitment problems, will be investigated in the future work, with special focuses on enhancing the convergence performance and achieving good enough solutions in a reasonable computational time. For non-convex power systems problems, the computational time of individual subsystems could be more significant as compared to the DC-OPF problem. The future work will investigate approaches for leveraging the number of iterations and the computational time of individual subsystems, and explore the asynchronous feature of distributed algorithms for enhancing the computational performance, especially when communication fault occurs or certain local controllers go offline.

## REFERENCES


[1] Z. Chen and L. Wu, "Residential appliance DR energy management with electric privacy protection by online stochastic optimization," *IEEE Trans. Smart Grid*, vol. 4, no. 4, pp. 1861–1869, Dec. 2013.

[2] Z. C. Zhao and L. Wu, "Impacts of high penetration wind generation and demand response on LMPs in day-ahead market," *IEEE Trans. Smart Grid*, vol. 5, no. 1, pp. 220–229, Jan. 2014.

[3] Z. C. Zhao, L. Wu, and G. H. Song, "Convergence of volatile power markets with price-based demand response," *IEEE Trans. Power Syst.*, vol. 29, no. 5, pp. 2107–2118, Sep. 2014.

[4] L. Wu, "Impact of price-based demand response on market clearing and locational marginal prices," *IET Gener. Transm. Distrib.*, vol. 7, no. 10, pp. 1087–1095, Oct. 2013.

[5] Z. Zhang and M.-Y. Chow, "Convergence analysis of the incremental cost consensus algorithm under different communication network topologies in a smart grid," *IEEE Trans. Power Syst.*, vol. 27, no. 4, pp. 1761–1768, Nov. 2012.

[6] G. Binetti, A. Davoudi, F. L. Lewis, D. Naso, and B. Turchiano, "Distributed consensus-based economic dispatch with transmission losses," *IEEE Trans. Power Syst.*, vol. 29, no. 4, pp. 1711–1720, Jul. 2014.

[7] W. T. Elsayed and E. F. El-Saadany, "A fully decentralized approach for solving the economic dispatch problem," *IEEE Trans. Power Syst.*, vol. 30, no. 4, pp. 2179–2189, Jul. 2015.

[8] F. Zhao, E. Litvinov, and T. X. Zheng, "A marginal equivalent decomposition method and its application to multi-area optimal power flow problems," *IEEE Trans. Power Syst.*, vol. 29, no. 1, pp. 53–61, Jan. 2014.

[9] A. Kargarin and Y. Fu, "System of systems based security-constrained unit commitment incorporating active distribution grids," *IEEE Trans. Power Syst.*, vol. 29, no. 5, pp. 2489–2498, Sep. 2014.

[10] D. T. Phan and X. A. Sun, "Minimal impact corrective actions in security-constrained optimal power flow via sparsity regularization," *IEEE Trans. Power Syst*., vol. 30, no. 4, pp. 1947–1956, Jul. 2015.

[11] E. Loukarakis, J. W. Bialek, and C. J. Dent, "Investigation of maximum possible OPF problem decomposition degree for decentralized energy markets," *IEEE Trans. Power Syst*., vol. 30, no. 5, pp. 2566–2578, Sep. 2015.

[12] Z. Zhang, N. Rahbari-Asr, and M.-Y. Chow, "Asynchronous distributed cooperative energy management through gossip-based incremental cost consensus," in *Proc. North Amer. Power Symp. (NAPS)*, Manhattan, KS, USA, 2011, pp. 1–6.

[13] A. J. Conejo and J. A. Aguado, "Multi-area coordinated decentralized DC optimal power flow," *IEEE Trans. Power Syst*., vol. 13, no. 4, pp. 1272–1278, Nov. 1998.

[14] P. N. Biskas, A. G. Bakirtzis, N. I. Macheras, and N. K. Pasialis, "A decentralized implementation of DC optimal power flow on a network of computers," *IEEE Trans. Power Syst*., vol. 20, no. 1, pp. 25–33, Feb. 2005.

[15] A. G. Bakirtzis and P. N. Biskas, "A decentralized solution to the DC-OPF of interconnected power systems," *IEEE Trans. Power Syst.*, vol. 18, no. 3, pp. 1007–1013, Aug. 2003.

[16] X. W. Lai, L. Xie, Q. Xia, H. W. Zhong, and C. Q. Kang, "Decentralized multi-area economic dispatch via dynamic multiplier-based Lagrangian relaxation," *IEEE Trans. Power Syst*., vol. 30, no. 6, pp. 3225–3233, Nov. 2015.

[17] G. Cohen, "Auxiliary problem principle and decomposition of optimization problems," *J. Optim. Theory Appl.*, vol. 32, no. 3, pp. 277–305, Nov. 1980.

[18] B. H. Kim and R. Baldick, "Coarse-grained distributed optimal power flow," *IEEE Trans. Power Syst*., vol. 12, no. 2, pp. 932–939, May 1997.

[19] R. Baldick, B. H. Kim, C. Chase, and Y. Luo, "A fast distributed implementation of optimal power flow," *IEEE Trans. Power Syst*., vol. 14, no. 3, pp. 858–864, Aug. 1999.

[20] V. Kekatos and G. B. Giannakis, "Distributed robust power system state estimation," *IEEE Trans. Power Syst.*, vol. 28, no. 2, pp. 1617–1626, May 2013.

[21] T. Erseghe, D. Zennaro, E. Dall'Anese, and L. Vangelista, "Fast consensus by the alternating direction multipliers method," *IEEE Trans. Signal Process.*, vol. 59, no. 11, pp. 5523–5537, Nov. 2011.

[22] T. Erseghe, "Distributed optimal power flow using ADMM," *IEEE Trans. Power Syst*., vol. 29, no. 5, pp. 2370–2380, Sep. 2014.

[23] M. Kraning, E. Chu, J. Lavaei, and S. Boyd, "Dynamic network energy management via proximal message passing," *Found. Trends Optim.*, vol. 1, no. 2, pp. 70–122, 2013.

[24] E. Dall'Anese, H. Zhu, and G. B. Giannakis, "Distributed optimal power flow for smart microgrids," *IEEE Trans. Smart Grid*, vol. 4, no. 3, pp. 1464–1475, Sep. 2013.

[25] S. Boyd, N. Parikh, E. Chu, B. Peleato, and J. Eckstein, "Distributed optimization and statistical learning via the alternating direction method of multipliers," *Found. Trends Mach. Learn.*, vol. 3, no. 1, pp. 1–122, 2011.

[26] D. P. Bertsekas and J. N. Tsitsiklis, *Parallel and Distributed Computation: Numerical Methods*. Englewood Cliffs, NJ, USA: Prentice Hall, 1980.

[27] A. Ahmadi-Khatir, A. J. Conejo, and R. Cherkaoui, "Multi-area energy and reserve dispatch under wind uncertainty and equipment failures," *IEEE Trans. Power Syst.*, vol. 28, no. 4, pp. 4373–4383, Nov. 2013.

[28] F. J. Nogales, F. J. Prieto, and A. J. Conejo, "A decomposition methodology applied to the multi-area optimal power flow problem," *Ann. Oper. Res.*, vol. 120, nos. 1–4, pp. 99–116, 2003.

[29] C. Zhao, J. H. Wang, J.-P. Watson, and Y. P. Guan, "Multi-stage robust unit commitment considering wind and demand response uncertainties," *IEEE Trans. Power Syst.*, vol. 28, no. 3, pp. 2708–2717, Aug. 2013.

[30] T. Goldstein, B. O'Donoghue, S. Settzer, and R. Baraniuk"Fast alternating direction optimization methods," *SIAM J. Imag. Sci.*, vol. 7, no. 3, pp. 1588–1623, 2014.

[31] Y. Nesterov, "A method of solving a convex programming problem with convergence rate $O(1/k^2)$," *Soviet Math. Doklady*, vol. 27, no. 2, pp. 372–376, 1983.
[32] E. Ghadimi, A. Teixeira, I. Shames, and M. Johanson, "Optimal parameter selection for the alternating direction method of multipliers (ADMM): Quadratic problems," *IEEE Trans. Autom. Control*, vol. 60, no. 3, pp. 644–658, Mar. 2015.
[33] [Online]. Available: http://people.clarkson.edu/∼lwu/data/IEEE118_ADMM/, accessed Jan. 2016.
[34] L. Wu, M. Shahidehpour, and Z. Li, "Comparison of scenario-based and interval optimization approaches to stochastic SCUC," *IEEE Trans. Power Syst.*, vol. 27, no. 2, pp. 913–921, May 2012.
[35] B. Hu and L. Wu, "Robust SCUC considering continuous/discrete uncertainties and quick-start units: A two-stage robust optimization with mixed-integer recourse," *IEEE Trans. Power Syst.*, vol. 31, no. 2, pp. 1407–1419, Mar. 2016.

**Yamin Wang** (S'13) received the B.S. degree from Shandong University, China, in 2011, and the M.S. degree from Tianjin University, China, in 2014, both in electrical engineering. He is currently pursuing the Ph.D. degree with the ECE Department, Clarkson University, USA. His research interests include distributed optimization of power system and forecasting of renewable energy.

**Lei Wu** (SM'13) received the B.S. degree in electrical engineering and the M.S. degree in systems engineering from Xi'an Jiaotong University, China, in 2001 and 2004, respectively, and the Ph.D. degree in electrical engineering from the Illinois Institute of Technology, USA, in 2008. He is currently an Associate Professor with the ECE Department, Clarkson University. His research interests include power systems optimization and economics.

**Shouxiang Wang** (SM'12) received the B.S. and M.S. degrees from the Shandong University of Technology, Jinan, China, in 1995 and 1998, respectively, and the Ph.D. degree from Tianjin University, Tianjin, China, in 2001, all in electrical engineering. He is currently a Professor with the School of Electrical Engineering and Automation, Tianjin University. His main research interests are distributed generation, microgrid, and smart distribution system.